

Isobaric yield ratios in heavy-ion reaction, and symmetry energy of neutron-rich nuclei at intermediate energy

Chun-Wang MA* and Fang WANG

Department of Physics, Henan Normal University, Xinxiang, 453007 China

Yu-Gang MA†

*Shanghai Institute of Applied Physics,
Chinese Academy of Sciences, Shanghai, 201800 China*

Chan JIN‡

Institute of Biophysics, The Second Military Medical University, Shanghai, 200433 China

(Dated: November 15, 2018)

Abstract

The isobaric yield ratios of the fragments produced in the neutron-rich ^{48}Ca and ^{64}Ni projectile fragmentation are analyzed in the framework of a modified Fisher model. The correlations between the isobaric yield ratios (R) and the energy coefficients in the Weizsäcker-Beth semiclassical mass formula (the symmetry-energy term a_{sym} , the Coulomb-energy term a_c , and the pairing-energy term a_p) and the difference between the chemical potential of neutron and proton ($\mu_n - \mu_p$) are investigated. Simple correlations between $(\mu_n - \mu_p)/T$, a_c/T , a_{sym}/T , and a_p/T (where T is the temperature), and $\ln R$ are obtained. It is suggested that $(\mu_n - \mu_p)/T$, a_c/T , a_{sym}/T , and a_p/T of neutron-rich nuclei can be extracted using isobaric yield ratios for heavy-ion collisions at intermediate energies.

PACS numbers: 21.65.Cd, 21.65.Ef, 21.65.Mn, 25.70.Mn

* machunwang@126.com

† ygamma@sinap.ac.cn

‡ jinchan2010@yahoo.cn

I. INTRODUCTION

The construction of a new generation of radioactive nuclear beam facilities has stimulated much research into isospin physics [1]. In heavy-ion reactions at intermediate energy, multifragmentation of the reaction system is generally observed in violent collisions and there is evidence that both subsaturated and supersaturated densities can be explored in such collisions [2–4]. Work in this area has concentrated on exploring the nuclear equation of state (EOS) and the liquid-gas phase transition in nuclear matter [5–8]. Isotopic yields in heavy-ion collisions provide a good probe for studying the nature of the disassembling nuclear systems. Many studies on fragment emission have attempted to use fragment yield distributions, either singly or by comparison to those of similar reactions, to explore the symmetry energy of the emitting source at different densities and temperatures [2, 4, 6, 7, 9–20]. The nuclear symmetry energy of a finite nucleus is an important parameter in the EOS of an asymmetric nucleus and in various processes in astrophysics and nuclear astrophysics. But the symmetry energy is difficult to measure experimentally and there are large differences in the theoretical results between different models and even within the same model with different parameters [1].

In a recent work analyzing isobaric yields [21], the ratio of the symmetry-energy coefficient to temperature, a_{sym}/T , as a function of fragment mass A was studied in a modified Fisher model (MFM) [22, 23]. The Coulomb-energy coefficient to temperature (a_c/T), and the pairing-energy to temperature (a_p/T) were also extracted at the same time. For the symmetry-energy term, the extracted values from experiments are in good agreement with those calculated for the final fragments in the ground states. The pairing effect is clearly observed in experiments and strongly supports the hypothesis that the observed effect originates at the end of the statistical cooling-down process of the excited fragments. A comparison between the Coulomb coefficients extracted experimentally and those calculated shows significant differences.

In this article, on the basis of the theory of a modified Fisher model [22, 23], which was adopted in Ref. [21], the correlation between the logarithm of the isobaric yield ratio $\ln R$ and a_{sym}/T , a_c/T , a_p/T and $(\mu_n - \mu_p)/T$ for fragments produced in 140 A MeV $^{48}\text{Ca} + ^9\text{Be}$ and $^{64}\text{Ni} + ^9\text{Be}$ reactions (experimental data are taken from Refs. [24, 25]) are analyzed. Coefficients of the volume energy, the surface energy, the Coulomb energy, the

symmetry energy and the pairing energy in the Weiszäcker-Beth semiclassical mass formula and $(\mu_n - \mu_p)/T$ for fragments will be extracted using these correlations.

II. ISOBARIC YIELD RATIOS IN THE MODIFIED FISHER MODEL

Following the modified Fisher model theory [6, 22, 23], the yield of fragment with mass number A and $I = N - Z$, $Y(A, I)$ is given by

$$Y(A, I) = CA^{-\tau} \exp\{[W(A, I) + \mu_n N + \mu_p Z]/T + N \ln(N/A) + Z \ln(Z/A)\}, \quad (1)$$

where C is a constant. The $A^{-\tau}$ term originates from the entropy of the fragment, and the last two terms are from the entropy contributions for the mixing of two substances in the Fisher droplet model [26]. μ_n and μ_p are the neutron and proton chemical potentials, respectively, and $W(A, I)$ is the free energy of the cluster at temperature T . $W(A, I)$ is given by the generalized Weiszäcker-Beth semiclassical mass formula [27, 28] at a given temperature T and density ρ :

$$W(A, I) = -E_{sym} - a_c(\rho, T)Z(Z-1)/A^{1/3} + a_v(\rho, T)A - a_s(\rho, T)A^{2/3} - \delta(N - Z), \quad (2)$$

where the indices v, s, c , and sym represent volume, surface, Coulomb, and symmetry energies, respectively. The symmetry energy E_{sym} , can be divided into a volume-symmetry term S_v and a surface-symmetry term S_s , i.e. $E_{sym} = S_v(\rho, T) + S_s(\rho, T)$, in which $S_v(\rho, T) = a_{vsym}(\rho, T)I^2/A$ and $S_s(\rho, T) = a_{ssym}(\rho, T)I^2 A^{2/3}$ [29, 30]. Following the semiempirical mass formulas, the pairing energy $\delta(N, Z)$ is given by [31]

$$\delta(N, Z) = \begin{cases} a_p(\rho, T)/A^{1/2} & \text{(odd-odd),} \\ 0 & \text{(even-odd),} \\ -a_p(\rho, T)/A^{1/2} & \text{(even-even),} \end{cases} \quad (3)$$

The yield ratio for fragments, $R(I + 2, I, A)$, between isobars differing by 2 units in I is defined as

$$\begin{aligned} R(I + 2, I, A) &= Y(A, I + 2)/Y(A, I) \\ &= \exp\{[W(I + 2, A) - W(I, A) + (\mu_n - \mu_p)]/T + S_{mix}(I + 2, A) - S_{mix}(I, A)\}, \end{aligned} \quad (4)$$

where $S_{mix}(I, A) = N \ln(N/A) + Z \ln(Z/A)$. To simplify the description, the density and temperature dependence of the coefficients in Eq. (2) is written as $a_i = a_i(\rho, T)$ (where

$i = v, s, c, ssym, vsym$ and p represent the volume energy, the surface energy, the Coulomb energy, the surface-symmetry energy, the volume symmetry energy, and the pairing energy, respectively). The temperature dependence of a_i at low T has been studied [29].

Inserting Eq. (2) into Eq. (4), one gets

$$R(I + 2, I, A) = \exp\{[(\mu_n - \mu_p) - 4a_{ssym}(I + 1)/A + 2a_c(Z - 1)/A^{1/3} - \delta(N + 1, Z - 1) + \delta(N, Z)]/T + \Delta(I + 2, I, A)\}, \quad (5)$$

where $\Delta(I + 2, I, A) = S_{mix}(I + 2, A) - S_{mix}(I, A)$. Similarly, one can define the fragment yield ratio $R(I + 4, I, A)$ between isobars differing by 4 units in I following Eq. (4) as

$$R(I + 4, I, A) = Y(A, I + 4)/Y(A, I) = \exp\{[W(I + 4, A) - W(I, A) + 2(\mu_n - \mu_p)]/T + S_{mix}(I + 4, A) - S_{mix}(I, A)\}, \quad (6)$$

and inserting Eq. (2) into Eq. (6), one gets

$$R(I + 4, I, A) = \exp\{[2(\mu_n - \mu_p) - 8a_{ssym}(I + 2)/A + 2a_c(2Z - 3)/A^{1/3} - \delta(N + 2, Z - 2) + \delta(N, Z)]/T + \Delta(I + 4, I, A)\}. \quad (7)$$

Equations (6) and (7) assume that a_s and a_v are the same for isobars, and omit the surface-symmetry-energy term as Ref. [21]. In this case, a_{vsym} is written as a_{ssym} according to Ref. [21].

For isobars with $I = -1$ and $I = 1$ (which are mirror nuclei), $\Delta(1, -1, A) = 0$, and the contributions from the symmetry term and the mixing entropy term in Eq. (5) drop out and, the pairing term also cancels out because these isobars are even-odd nuclei. Taking the logarithm of the resultant equation, one obtains

$$\ln[R(1, -1, A)] = [(\mu_n - \mu_p) + 2a_c(Z - 1)/A^{1/3}]/T. \quad (8)$$

Following Eq. (4), an isobar with odd " I " is an odd-even nucleus and the pairing energy is zero, so one gets

$$\ln[R(I + 2, I, A)] = [(\mu_n - \mu_p) - 8a_{ssym}/A + 2a_c(Z - 1)/A^{1/3}]/T + \Delta(I + 2, I, A). \quad (9)$$

Considering ratios of isobars with " $I-2$ ", " I ", and " $I+2$ ", and assuming isobars with " I " in $R(I, I - 2, A)$ and isobars with $I+2$ in $R(I + 2, I, A)$ are isotopes, one can reach

$$(8a_{ssym}/A + 2a_c/A^{1/3})/T = \ln[R(I, I - 2, A)] - \ln[R(I + 2, I, A)] - \Delta(I, I - 2, A) + \Delta(I + 2, I, A). \quad (10)$$

In Eq. (10), isobars with " $I-2$ " are taken as the reference nuclei.

Following Eq. (6) and taking isobars with " I " as the reference nuclei, one gets

$$\ln[R(I+4, I, A)] = [(\mu_n - \mu_p) - 8(I+2)a_{sym}/A + 2a_c(2Z-3)/A^{1/3}]/T + \Delta(I+4, I, A). \quad (11)$$

Taking isobars with " $I-2$ " as the reference nuclei, the difference between $2\ln[R(I+2, I, A)]$ and $\ln[R(I+4, I, A)]$ can be written as

$$(8a_{sym}/A + 2a_c/A^{1/3})/T = \ln[R(I+2, I, A)] - \ln[R(I+4, I, A)] - \Delta(I+2, I, A) + \Delta(I+4, I, A). \quad (12)$$

It can be found that

$$\begin{aligned} & \ln[R(I+2, I, A)] - \ln[R(I+4, I, A)] + \ln[R(I+4, I+2, A)] \\ & - \Delta(I+4, I+2, A) - \Delta(I+2, I, A) + \Delta(I+4, I, A) = 0. \end{aligned} \quad (13)$$

Similarly, taking isobars with " $I-2$ " as the reference nuclei, the difference between $2\ln[R(I, I-2, A)] - \ln[R(I+2, I, A)]$ reads

$$[(\mu_n - \mu_p) + 2a_c Z/A^{1/3}]/T = 2\ln[R(I, I-2, A)] - \ln[R(I+2, I, A)] - 2\Delta(I, I-2, A) + \Delta(I, I+2, A). \quad (14)$$

In Ref. [21], $[(\mu_n - \mu_p)]/T$ for different reaction systems is expressed as $[(\mu_n - \mu_p)/T]_i = [(\mu_n - \mu_p)/T]_0 + \Delta\mu(Z/A)/T$, in which $(Z/A) = (Z_p + Z_t)/(A_p + A_t)$, and p and t represent the projectile and the target nuclei. Taking one reaction system as the reference and fitting the different reaction systems, $\Delta\mu(Z/A)/T$ for each reaction system can be fixed. Then a_{sym}/T and a_c/T are extracted from the values of $(\mu_n - \mu_p)/T$ for each reaction system. Here, a_{sym}/T , a_c/T and $(\mu_n - \mu_p)/T$ can be extracted using Eq. (10), (12), and (14) only for one projectile fragmentation reaction.

Using Eq. (8), (10), (12), and (14), we analyze the yield ratios of isobars produced in the 140A MeV $^{48}\text{Ca} + ^9\text{Be}$ and $^{64}\text{Ni} + ^9\text{Be}$ reactions [24, 25]. In Fig. 1 and 2, the correlations between $\ln[R(I, I-2, A)] - \ln[R(I+2, I, A)]$ and the mass number (A) of fragments [Eq. (10)], and the correlations between $\ln[R(I+2, I, A)] - \ln[R(I+4, I, A)]$ and A of fragments [Eq. (12)] are plotted. These correlations are fitted using a function $y = (8a_{sym}/A + 2a_c/A^{1/3})/T$, in which A is the argument and a_{sym}/T and a_c/T are parameters. The values for $\ln[R(1, -1, A)] - \ln[R(3, 1, A)]$ shows a large difference to the values for $\ln[R(I, I-2, A)] - \ln[R(I+2, I, A)]$. For isobars with $I \geq 3$, the values for $\ln[R(I, I-2, A)] - \ln[R(I+2, I, A)]$ overlap.

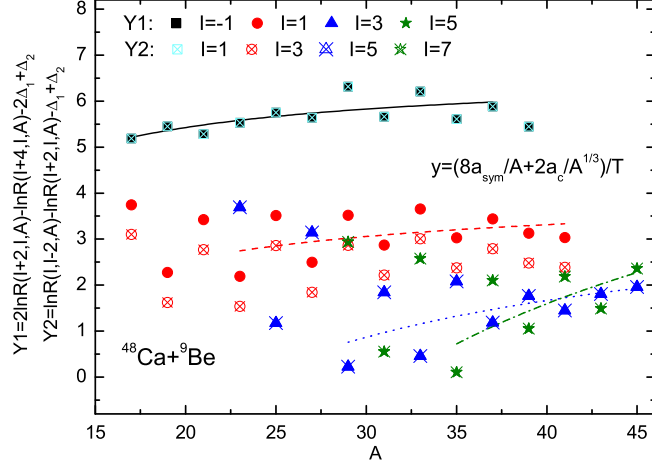


FIG. 1. (Color online) Correlations between $(8a_{sym}/A + 2a_c/A^{1/3})/T$ for different isobars with I and A of fragments in the 140 A MeV $^{48}\text{Ca} + ^9\text{Be}$ reaction. The lines are the fitting results using Eq. (10).

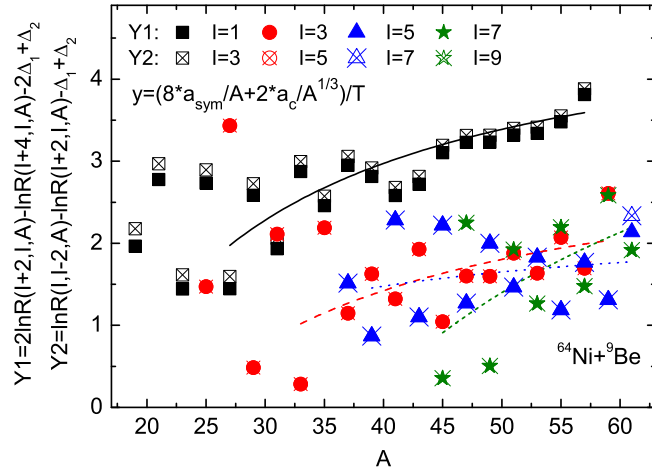


FIG. 2. (Color online) Correlations between $(8a_{sym}/A + 2a_c/A^{1/3})/T$ for different isobars with I and A of fragments in the 140 A MeV $^{64}\text{Ni} + ^9\text{Be}$ reaction. The lines are the fitting results using Eq. (10).

In Fig. 3 and 4, the correlations between $2\ln[R(I, I - 2, A)] - \ln[R(I + 2, I, A)]$ and $2Z/A^{1/3}$ of isobars (using Eq. 14) are depicted. The correlations are fitted using a function $y = [(\mu_n - \mu_p) + 2a_c Z/A^{1/3}]/T$. The values for $[(\mu_n - \mu_p) + 2a_c Z/A^{1/3}]/T$ for isobars with "I=-1" and "I = 1" shows large differences, but these decrease and there is an overlap as I increases.

In Fig. 5, the correlations between $\ln[R(1, -1, A)] - \ln[R(I + 2, I, A)]$ for isobars with I

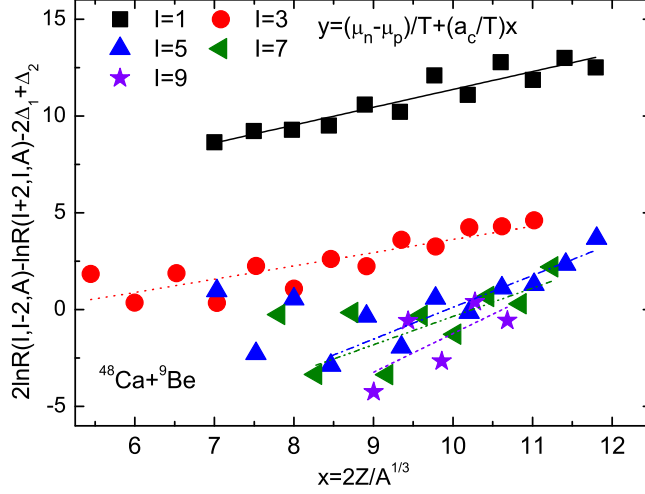


FIG. 3. (Color online) Correlations between $2\ln[R(I, I - 2, A)] - \ln[R(I + 2, I, A)]$ and $2Z/A^{1/3}$ of fragments produced in the 140 A MeV $^{48}\text{Ca} + ^9\text{Be}$ reaction. The lines are the fitting results using Eq. (14).

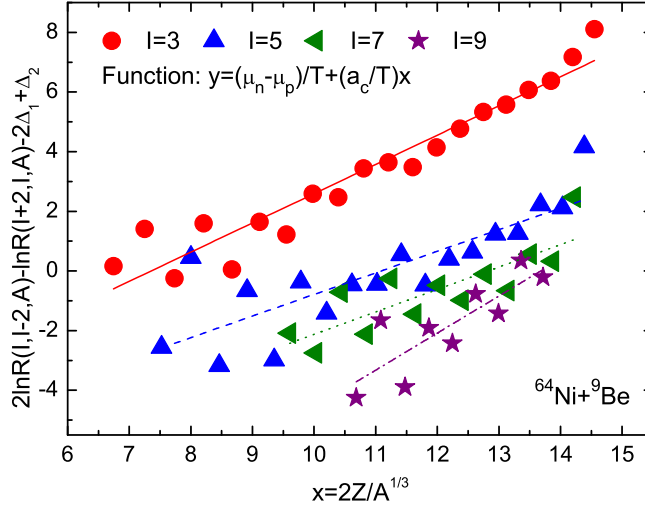


FIG. 4. (Color online) Correlations between $2\ln[R(I, I - 2, A)] - \ln[R(I + 2, I, A)]$ and $2Z/A^{1/3}$ of fragments produced in the 140 A MeV $^{64}\text{Ni} + ^9\text{Be}$ reaction. The lines are the fitting results using Eq. (14).

and $2Z/A^{1/3}$ (using Eq. (15)) for fragments are displayed. The correlations are fitted using Eq. (14). The values for $[(\mu_n - \mu_p) + 2a_c Z/A^{1/3}]/T$ for isobars with " $I = -1$ " and " $I = 1$ " show large differences, but these decreases and there is an overlap as I increases.

Omitting the difference between $(\mu_n - \mu_p)/T$ for nuclei with different I , and taking isobars with " $I = -1$ " as the reference nuclei, the difference between $\ln[R(1, -1, A)] - \ln[R(I+2, I, A)]$

can be written as

$$(8Ia_{asym}/A + 2a_c/A^{1/3})/T = \ln[R(1, -1, A)] - \ln[R(I + 2, I, A)] + \Delta(I, I + 2, A). \quad (15)$$

In Fig. 5, the correlations between $\ln[R(1, -1, A)] - \ln[R(I + 2, I, A)]$ for isobars with different I and A for fragments are plotted. The correlations are fitted using Eq. (15). The values for $\ln[R(1, -1, A)] - \ln[R(I + 2, I, A)]$ for different isobars increase as the I of isobars increases.

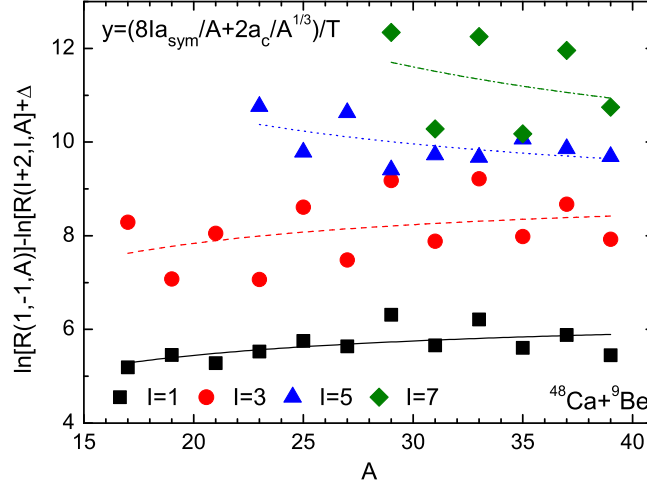


FIG. 5. (Color online) Correlations between $\ln[R(1, -1, A)] - \ln[R(I + 2, I, A)]$ for isobars with different I and A of fragments in the 140 A MeV $^{48}\text{Ca} + ^9\text{Be}$ reactions. The lines are the fitting results using Eq. (15).

Following the same methods in Ref. [21], the pairing term a_p/T for isobars with $I=0$ and $I=2$ are rewritten here:

$$a_p/T \sim (sgn)\frac{1}{2}A^{1/2}\{\ln[R(2, 0, A)] - \frac{1}{2}\{\ln[R(1, -1, A)] + \ln[R(3, 1, A)] - \Delta(3, 1, A)\} - \Delta(2, 0, A)\}, \quad (16)$$

and for isobars with $I = 2$ and $I = 4$,

$$a_p/T \sim (sgn)\frac{1}{2}A^{1/2}\{\ln[R(4, 2, A)] - \frac{1}{2}\{\ln[R(1, -1, A)] - 3\ln[R(3, 1, A)] + 3\Delta(3, 1, A)\} - \Delta(4, 2, A)\}. \quad (17)$$

Similarly, one can have

$$a_p/T \sim (sgn)\frac{1}{2}A^{1/2}\{\ln[R(2, 0, A)] - \frac{1}{2}\{\ln[R(1, -1, A)] - 3\ln[R(3, 1, A)] + \Delta(3, 1, A)\} - \Delta(2, 0, A)\} \quad (18)$$

and for isobars with $I = 2$ and $I = 4$,

$$a_p/T \sim (sgn) \frac{1}{2} A^{1/2} \{ \ln[R(4, 2, A)] - \frac{1}{2} \{ \ln[R(3, 1, A)] - 3 \ln[R(5, 3, A)] \} - \Delta(3, 1, A) + 3 \Delta(5, 3, A) \} - \Delta(4, 2, A), \quad (19)$$

and

$$a_p/T \sim (sgn) \frac{1}{2} A^{1/2} \{ \ln[R(4, 2, A)] - \frac{1}{2} \{ \ln[R(3, 1, A)] + \ln[R(5, 3, A)] \} + \Delta(3, 1, A) + \Delta(5, 3, A) \} - \Delta(4, 2, A). \quad (20)$$

For an (odd,odd) nucleus $sgn = 1$ and for an (even,even) nucleus $sgn = -1$. The approximations assumed in Eq.(16) and (17) are $(\mu_n - \mu_p)/T$, a_{sym}/T and a_c/T in $\ln[R(3, 1, A)]$ and $\ln[R(4, 2, A)]$ and are the same as those in $\ln[R(1, -1, A)]$. Similar approximations are made in Eq. (18), (19) and (20). In Fig. 6, correlations between a_p/T and A of fragments produced in the 140 A MeV $^{48}\text{Ca} + ^9\text{Be}$ reactions are plotted. a_p/T of isobars with $I = 0$ and $I = 2$ are extracted using Eq. (16)-(20), respectively. In Eq.(16), the chemical term, symmetry term and Coulomb term of $R(2, 0, A)$ are assumed to be equal to those of $R(1, -1, A)$. In Eq. (18), $(\mu_n - \mu_p)/T$, a_{sym}/T and a_c/T of $R(2, 0, A)$ are assumed to be equal to those of $R(3, 1, A)$. For (even,even) isobars with $I=0$ and $I=2$, the extracted a_p/T using Eq. (16) is bigger than that using Eq. (18), while for (odd,odd) isobars the extracted a_p/T using Eq. (16) are smaller than those using Eq. (18).

Due to lack of data for cross sections of mirror nuclei in the ^{64}Ni projectile fragmentation, figures like Figs. 5 and 6 are not plotted for ^{64}Ni . From Figs. 1 to 6, it can be seen that the correlations between isobaric yield ratios and $(\mu_n - \mu_p)/T$, a_{sym}/T , a_c/T , and a_p/T can fit the measured data well. But for isobars with big I , there are not enough data to form chains and it is impossible to extract the values for a_{sym}/T and a_c/T for these very neutron-rich isobars.

The method discussed above has the great advantage that the analysis can be performed in a single reaction and there is no need to calibrate $\Delta\mu(Z/A)$ as in Ref. [21]. The extracted values of $(\mu_n - \mu_p)/T$, a_{sym}/T , a_c/T , and a_p/T are at a specific temperature associated with the incident energy. $(\mu_n - \mu_p)/T$, a_{sym}/T , a_c/T , and a_p/T are all temperature dependent. To study the dependence of $(\mu_n - \mu_p)/T$, a_{sym}/T , a_c/T , and a_p/T on temperature, projectile fragmentation at different energies should be investigated.

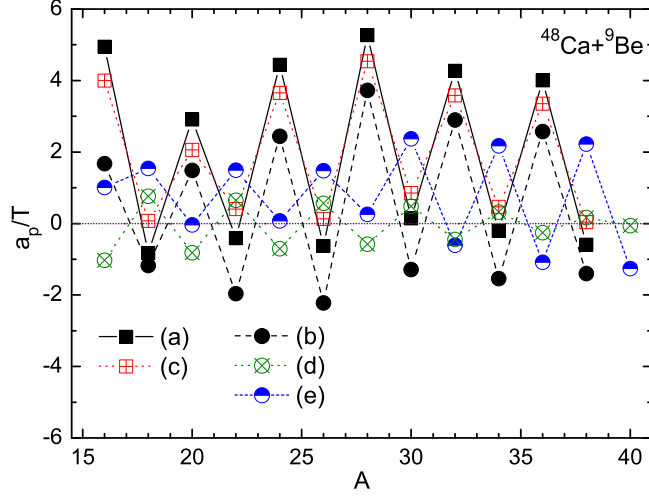


FIG. 6. (Color online) Correlations between a_p/T and A for fragments produced in the 140 A MeV $^{48}\text{Ca} + ^9\text{Be}$ reaction. (a), (b), (c), (d), and (e) are results obtained using Eqs. (16), (17), (18), (19), and (20), respectively.

III. SUMMARY

In summary, the coefficients of the Coulomb energy a_c/T , symmetry energy a_{sym}/T , pairing energy a_p/T , and $(\mu_n - \mu_p)/T$ have been studied by analyzing the yield ratios (R) of isobars in projectile fragmentation in the framework of the modified Fisher model. Very simple correlations between $(\mu_n - \mu_p)/T$, a_c/T , a_{sym}/T , a_p/T , and R are obtained. It is found that these correlations can fit the experimental results well and can be used to extract the symmetry energy of the neutron-rich nuclei.

ACKNOWLEDGMENTS

This work is partially supported by the National Natural Science Foundation of China under Contract No. 10905017, and No. 11035009, the Program for Innovative Research Team (in Science and Technology) under Grant No. 2010IRTSTHN002 in the University of Henan Province, China, and the Shanghai Development Foundation for Science and Technology under Contract No. 09JC1416800, and the Knowledge Innovation Project of the

- [1] B.-A. Li, L.-W. Chen, C. M. Ko, et al., Phys. Rep. **464**, 113 (2008).
- [2] S. Kowalski, J. B. Natowitz, S. Shlomo, et al., Phys. Rev. C **75**, 014601 (2007).
- [3] B. A. Li, Phys. Rev. C **67**, 017601 (2003).
- [4] Y. G. Ma, Q. M. Su, W. Q. Shen et al., Phys. Rev. C **60**, 024607 (1999).
- [5] A. Bonasera et al., Phys. Rev. Lett. **101**, 122702 (2008).
- [6] C. B. Das, S. D. Gupta, W. G. Lynch, Phys. Rep. **406**, 1 (2005).
- [7] S. Das Gupta, A. Z. Mekjian and M. B. Tsang, Advances in Nuclear Physics **26**, 89 (2002).
- [8] A. L. Goodman, J. I. Kapusta, A. Z. Mekjian, Phys. Rev. C **30**, 851 (1984).
- [9] H. S. Xu et al., Phys. Rev. Lett. **85**, 716 (2000).
- [10] M. B. Tsang et al., Phys. Rev. C **64**, 054615 (2001).
- [11] A. S. Botvina, O. V. Lozhkin, and W. Trautmann, Phys. Rev. C **65**, 044610 (2002).
- [12] A. Ono, P. Danielewicz, W. A. Friedman et al., Phys. Rev. C **68**, 051601(R) (2003).
- [13] Y. G. Ma, J. B. Natowitz, R. Wada et al., Phys. Rev. C **71**, 054606 (2005).
- [14] Y. G. Ma, A. Siwek, J. Péter et al., Phys. Lett. B **390**, 41 (1997).
- [15] D. Q. Fang, Y. G. Ma, C. Zhong, et al., J. Phys. G: Nucl. Part. Phys., **34** (2007) 2173.
- [16] C. W. Ma, Y. Fu, D. Q. Fang et al., Chin. Phys. B, **17**, (2008) 1216.
- [17] D. Q. Fang, Y. G. Ma, X. Z. Cai et al., Phys. Rev. C, **81**, 047603 (2010).
- [18] X. Y. Sun, D. Q. Fang, Y. G. Ma et al., Phys. Lett. B **687**, 396 (2010).
- [19] C. W. Ma, H. L. Wei, J. Y. Wang et al., Phys. Rev. C **79**, 034606 (2009).
- [20] C. W. Ma, Y. Fu, D. Q. Fang et al., Int. J. Mod. Phys. E **17**, 1669 (2008).
- [21] M. Huang, Z. Chen, S. Kowalski et al., Phys. Rev. C **81**, 044620 (2010).
- [22] R. W. Minich, S. Agarwal, A. Bujak et al., Phys. Lett. B **118**, 458 (1982).
- [23] A. S. Hirsch, A. Bujak, J. E. Finn et al., Nucl. Phys. A **418**, 267c (1984).
- [24] M. Mocko, M. B. Tsang, D. Lacroix et al., Phys. Rev. C **78**, 024612 (2008).
- [25] M. Mocko, M. B. Tsang, L. Andronenko et al., Phys. Rev. C **74**, 054612 (2006).
- [26] M. E. Fisher, Rep. Prog. Phys. **30**, 615 (1967).
- [27] C. F. von Weizsäcker, Z. Phys. **96**, 431 (1935).
- [28] H. A. Bethe, Rev. Mod. Phys. **8**, 82 (1936).

- [29] S. J. Lee, and A. Z. Mekjian, Phys. Rev. C **82**, 064319 (2010).
- [30] N. Nikolov, N. Schunck, W. Nazarewicz, et. al., Phys. Rev. C **83**, 034305 (2011).
- [31] A. E. S. Green and D. F. Edwards, Phys. Rev. **91**, 46 (1953).